

Nuclear structure in Parity Doublet Model

Myeong-Hwan Mun,¹ Ik Jae Shin,² Won-Gi Paeng,² Masayasu Harada,^{3,4,5} and Youngman Kim⁶

¹*Department of Physics and Origin of Matter and Evolution of Galaxy Institute, Soongsil University, Seoul 06978, Korea*

²*Rare Isotope Science Project, Institute for Basic Science, Daejeon 34000, Korea*

³*Department of Physics, Nagoya University, Nagoya, 464-8602, Japan*

⁴*Kobayashi-Maskawa Institute for the Origin of Particles and the Universe, Nagoya University, Nagoya, 464-8602, Japan*

⁵*Advanced Science Research Center, Japan Atomic Energy Agency, Tokai 319-1195, Japan*

⁶*Center for Exotic Nuclear Studies, Institute for Basic Science, Daejeon 34126, Korea*

(Dated: July 7, 2023)

Using an extended parity doublet model with the hidden local symmetry, we study some properties of nuclei in the mean field approximation to see if the parity doublet model could reproduce nuclear properties and also to estimate the value of the chiral invariant nucleon mass m_0 preferred by nuclear structure. We first determine our model parameters using the inputs from free space and from nuclear matter properties. Then, we study some basic nuclear properties such as the nuclear binding energy with several different choices of the chiral invariant mass. We observe that our results approach the experimental values as m_0 is increased until $m_0 = 700$ MeV and start to deviate more from the experiments afterwards with m_0 larger than $m_0 = 700$ MeV. From this observation, we conclude that $m_0 = 700$ MeV is preferred by nuclear properties. We then calculate some properties of several selected nuclei with $m_0 = 700$ MeV and compare them with experiments. Finally, we study the neutron-proton mass difference in some nuclei.

I. INTRODUCTION

Nuclei are interesting and important quantum finite many-body systems, providing a solid testing ground for our understanding of the strong interactions and many-body techniques. In principle, we should be able to understand nuclei in terms of quarks and gluons in the framework of quantum chromodynamics (QCD). For instance, it will be especially interesting to investigate how QCD vacuum properties are reflected in the properties of nuclear matter and finite nuclei. This is, however, a formidable task to achieve due to the non-perturbative nature of the strong interaction at low energies. Since the nucleus is commonly believed to be composed of the protons and neutrons and it is highly nontrivial to understand nuclei in terms of quarks and gluons in the framework of QCD, it is natural to view the nucleus as a collection of interacting protons and neutrons. In addition, in the light of effective theory, thanks to the QCD separation scale due to confinement or spontaneous chiral symmetry breaking, using protons and neutrons as relevant degrees of freedom for nuclei would be still desirable.

Studying the origin of hadron masses is one of important problems in nuclear physics. As it is well known, the current quark mass could explain roughly 2% of the nucleon mass. A picture in nuclear physics is that the nucleon mass in the chiral limit could be explained by quark-antiquark condensates in QCD vacuum, i.e., spontaneous chiral symmetry breaking. In the parity doublet model [1], however, the nucleon mass has a piece called the chiral invariant mass m_0 that may have something to do with QCD trace anomaly. In Ref. [1], from the decay of N^* , $N^*(1535) \rightarrow N + \pi$, the value of the chiral invariant mass m_0 was determined as $m_0 = 270$ MeV.

Dense matter, which is intimately related to heavy ion collisions, nuclear structure and neutron stars, has been

extensively investigated in the parity doublet models [2–10], while nuclear structure study in parity doublet models has not been made. In Ref. [3], the chiral invariant mass was estimated as $m_0 \sim 800$ MeV from nuclear matter properties, especially incompressibility. In Ref. [6], the chiral invariant mass m_0 was re-expressed as the sum of the contributions from tetraquark and gluon condensates. An extended parity doublet model [10] reasonably reproduces the properties of nuclear matter with the chiral invariant nucleon mass in the range from 500 to 900 MeV. As discussed in Ref. [11], it is expected that a larger m_0 implies a smaller Yukawa coupling of the σ field to nucleons, since a part of the nucleon mass from the chiral symmetry breaking is smaller. The attractive force by the σ should be balanced by the repulsive force mediated by ω at the saturation density, so that the ω contribution is smaller for large m_0 . In the higher density region, ω contribution is expected to grow while σ contribution decreases. As a result of the repulsive nature of the ω , the equation of state is softer for large m_0 [11].

A promising microscopic theoretical tool for nuclear matter and (medium-mass and heavy) nuclei is energy density functional (EDF) theory [12]. With a few parameters, density functional theory provides a successful description of ground-state properties of spherical and deformed nuclei. Self-consistent relativistic mean field theory is a useful method to obtain the covariant energy density functionals. The covariant EDF includes the nucleon spin degree of freedom naturally and, therefore, can consistently explain the nuclear spin-orbit potential. For the details of covariant EDF, we refer to Refs. [13–16].

In this work, using the parity doublet model developed in Ref. [10], we study the properties of nuclei in self-consistent relativistic mean field theory to see if a parity doublet model works for nuclear properties and to find out the value of the chiral invariant mass preferred by

nuclear structures. As a first attempt, we will focus on the properties of stable nuclei in the present study.

The extended parity doublet model [10], where the chiral invariant nucleon mass is in the range from 500 to 900 MeV, is briefly described in Section II and the results are given in Section III. We then summarize the present work in Section IV.

II. PARITY DOUBLET MODEL WITH HIDDEN LOCAL SYMMETRY

In this section we study finite nuclei in the context of the parity doublet model [1, 17–19]. To investigate nuclear matter or finite nuclei using a parity doublet model, either isospin symmetric or asymmetric, one needs to introduce vector mesons in the model. A convenient way to do that, which respects chiral symmetry, is to use the Hidden Local Symmetry (HLS) [20, 21]. In Ref. [10], a parity doublet model with the HLS was constructed for an asymmetric nuclear matter study. It was shown in Ref. [10] that the phase structure of cold dense matter depends on the value of the chiral invariant mass and also on isospin asymmetry. In this section, we use the extended parity doublet model constructed in Ref. [10].

We start with the Lagrangian,

$$\begin{aligned} \mathcal{L} = & \bar{\psi}_1 i \not{\partial} \psi_1 + \bar{\psi}_2 i \not{\partial} \psi_2 + m_0 (\bar{\psi}_2 \gamma_5 \psi_1 - \bar{\psi}_1 \gamma_5 \psi_2) \\ & + g_1 \bar{\psi}_1 (\sigma + i \gamma_5 \vec{\tau} \cdot \vec{\pi}) \psi_1 + g_2 \bar{\psi}_2 (\sigma - i \gamma_5 \vec{\tau} \cdot \vec{\pi}) \psi_2 \\ & - g_{\omega NN} \bar{\psi}_1 \gamma_\mu \omega^\mu \psi_1 - g_{\omega NN} \bar{\psi}_2 \gamma_\mu \omega^\mu \psi_2 \\ & - g_{\rho NN} \bar{\psi}_1 \gamma_\mu \vec{\rho}^\mu \cdot \vec{\tau} \psi_1 - g_{\rho NN} \bar{\psi}_2 \gamma_\mu \vec{\rho}^\mu \cdot \vec{\tau} \psi_2 \\ & - e \bar{\psi}_1 \gamma^\mu A_\mu \frac{1 - \tau_3}{2} \psi_1 - e \bar{\psi}_2 \gamma^\mu A_\mu \frac{1 - \tau_3}{2} \psi_2 + \mathcal{L}_M \end{aligned} \quad (1)$$

where the baryon fields ψ_1 and ψ_2 transform as

$$\begin{aligned} \psi_{1R} & \rightarrow R \psi_{1R}, & \psi_{1L} & \rightarrow L \psi_{1L}, \\ \psi_{2R} & \rightarrow L \psi_{2R}, & \psi_{2L} & \rightarrow R \psi_{2L}, \end{aligned} \quad (2)$$

with L and R being the elements of $SU(2)_L$ and $SU(2)_R$ chiral symmetry group, respectively. The meson part of Lagrangian is given by

$$\begin{aligned} \mathcal{L}_M = & \frac{1}{2} \partial_\mu \sigma \partial^\mu \sigma + \frac{1}{2} \partial_\mu \vec{\pi} \cdot \partial^\mu \vec{\pi} \\ & - \frac{1}{4} \Omega_{\mu\nu} \Omega^{\mu\nu} - \frac{1}{4} \vec{R}_{\mu\nu} \cdot \vec{R}^{\mu\nu} - \frac{1}{4} F_{\mu\nu} F^{\mu\nu} \\ & + \frac{\bar{\mu}^2}{2} (\sigma^2 + \vec{\pi}^2) - \frac{\lambda}{4} (\sigma^2 + \vec{\pi}^2)^2 + \frac{\lambda_6}{6} (\sigma^2 + \vec{\pi}^2)^3 + \epsilon \sigma \\ & + \frac{1}{2} m_\omega^2 \omega_\mu \omega^\mu + \frac{1}{2} m_\rho^2 \vec{\rho}_\mu \cdot \vec{\rho}^\mu \end{aligned} \quad (3)$$

with

$$\begin{aligned} \Omega_{\mu\nu} & = \partial_\mu \omega_\nu - \partial_\nu \omega_\mu, \\ \vec{R}_{\mu\nu} & = \partial_\mu \vec{\rho}_\nu - \partial_\nu \vec{\rho}_\mu, \\ F_{\mu\nu} & = \partial_\mu A_\nu - \partial_\nu A_\mu. \end{aligned} \quad (4)$$

In this work, we adopt a mean field approximation and consider the following mean fields for mesons: $\sigma \rightarrow \langle \sigma \rangle$,

$\omega_\mu \rightarrow \delta_{\mu 0} \langle \omega_0 \rangle$, and $\rho_{i\mu} \rightarrow \delta_{i3} \delta_{\mu 0} \langle \rho_0^3 \rangle$. The pion mass m_π , σ meson mass m_σ , and pion decay constant f_π are given by

$$\begin{aligned} m_\pi^2 & = \lambda \langle \sigma \rangle^2 - \bar{\mu}^2 - \lambda_6 \langle \sigma \rangle^4, \\ m_\sigma^2 & = 3\lambda \langle \sigma \rangle^2 - \bar{\mu}^2 - 5\lambda_6 \langle \sigma \rangle^4, \\ f_\pi & = \langle \sigma \rangle. \end{aligned} \quad (5)$$

After diagonalization of the baryon mass terms, we get the mass of the nucleon field N , which corresponds to one of the mass eigenstates, as

$$m_N = \frac{1}{2} \left(\sqrt{(g_1 + g_2)^2 \langle \sigma \rangle^2 + 4m_0^2} - (g_1 - g_2) \langle \sigma \rangle \right). \quad (6)$$

The equations of motion (EoM) for the stationary mean fields $\tilde{\sigma}$, ω_0 , ρ_0^3 and A_0 read

$$\begin{aligned} \left(-\vec{\nabla}^2 + m_\sigma^2 \right) \langle \tilde{\sigma}(\vec{x}) \rangle & = -\bar{N}(\vec{x}) N(\vec{x}) \left. \frac{\partial m_N(\tilde{\sigma})}{\partial \tilde{\sigma}} \right|_{\tilde{\sigma}=\langle \tilde{\sigma}(\vec{x}) \rangle} \\ & + (-3f_\pi \lambda + 10f_\pi^3 \lambda_6) \langle \tilde{\sigma}(\vec{x}) \rangle^2 \\ & + (-\lambda + 10f_\pi^2 \lambda_6) \langle \tilde{\sigma}(\vec{x}) \rangle^3 \\ & + 5f_\pi \lambda_6 \langle \tilde{\sigma}(\vec{x}) \rangle^4 + \lambda_6 \langle \tilde{\sigma}(\vec{x}) \rangle^5, \end{aligned} \quad (7)$$

$$\left(-\vec{\nabla}^2 + m_\omega^2 \right) \langle \omega_0(\vec{x}) \rangle = g_{\omega NN} N^\dagger(\vec{x}) N(\vec{x}), \quad (8)$$

$$\left(-\vec{\nabla}^2 + m_\rho^2 \right) \langle \rho_0^3(\vec{x}) \rangle = g_{\rho NN} N^\dagger(\vec{x}) \tau^3 N(\vec{x}), \quad (9)$$

$$-\vec{\nabla}^2 \langle A_0(\vec{x}) \rangle = e N^\dagger(\vec{x}) \frac{1 - \tau_3}{2} N(\vec{x}). \quad (10)$$

Note here that for calculational handiness we take the shift $\sigma = f_\pi + \tilde{\sigma}$. Since we are interested in finite nuclei, we will not consider the EoM for the parity partner of the nucleon, $N^*(1535)$, which does not form its Fermi sea near the saturation density. In addition, since our primary goal here is to see if the parity doublet model can explain some basic nuclear properties such as the binding energy, we will not consider pairing correlations which are essential for odd-even staggering in nuclear properties. For instance, according to the semi-empirical mass formula, the contribution from the pairing term to the binding energy per nucleon of ^{58}Ni is only about 0.03 MeV.

The EoM for the nucleon is given by

$$[\vec{\alpha} \cdot \vec{p} + \beta m_N (\langle \tilde{\sigma}(\vec{x}) \rangle) + V(\vec{x})] N_i(\vec{x}) = \epsilon_i N_i(\vec{x}), \quad (11)$$

where N_i is the single-particle wave function and

$$V(\vec{x}) = g_{\omega NN} \langle \omega_0(\vec{x}) \rangle + g_{\rho NN} \langle \rho_0^3(\vec{x}) \rangle \tau^3 + e \frac{(1 - \tau_3)}{2} \langle A_0(\vec{x}) \rangle. \quad (12)$$

With assuming the spherical shape of the nucleus, we can solve the Eqs. (7)-(10) and Eq. (11) simultaneously to obtain the energy

$$E = \int d^3x \mathcal{H}(\vec{x}). \quad (13)$$

After subtracting out the vacuum contribution, we write the Hamiltonian density $\mathcal{H}(\vec{x})$ in the mean field approximation as

$$\begin{aligned}
\mathcal{H} = & \bar{N}(-i\gamma^i\partial_i + m_N)N + g_{\omega NN}\langle\omega_0\rangle N^\dagger N + g_{\rho NN}\langle\rho_0^3\rangle N^\dagger\tau^3 N + e\langle A_0\rangle N^\dagger\frac{1-\tau_3}{2}N \\
& -\frac{1}{2}\partial^i\langle\tilde{\sigma}\rangle\partial_i\langle\tilde{\sigma}\rangle + \frac{1}{2}\partial^i\langle\omega_0\rangle\partial_i\langle\omega_0\rangle + \frac{1}{2}\partial^i\langle\rho_0^3\rangle\partial_i\langle\rho_0^3\rangle + \frac{1}{2}\partial^i\langle A_0\rangle\partial_i\langle A_0\rangle \\
& -\frac{\bar{\mu}^2}{2}\left[(f_\pi + \langle\tilde{\sigma}\rangle)^2 - f_\pi^2\right] + \frac{\lambda}{4}\left[(f_\pi + \langle\tilde{\sigma}\rangle)^4 - f_\pi^4\right] - \frac{\lambda_6}{6}\left[(f_\pi + \langle\tilde{\sigma}\rangle)^6 - f_\pi^6\right] - \epsilon\langle\tilde{\sigma}\rangle \\
& -\frac{1}{2}m_\omega^2\langle\omega_0\rangle^2 - \frac{1}{2}m_\rho^2\langle\rho_0^3\rangle^2.
\end{aligned} \tag{14}$$

Then, the binding energy (BE) per nucleon is given by

$$\text{BE}/A = -\frac{E}{A} + m_N. \tag{15}$$

III. RESULTS

Following Ref. [10], we determine the free parameters in our model using the inputs in free space listed in Table I and nuclear matter properties. The nuclear matter

TABLE I. The inputs from free space (in MeV).

m_N	m_{N^*}	m_ω	m_ρ	f_π	m_π
939	1535	783	776	93	138

properties used to fix the parameters are given by

$$\begin{aligned}
\frac{E}{A} - m_N &= -16 \text{ MeV}, \quad n_0 = 0.16 \text{ fm}^{-3}, \\
K &= 240 \pm 40 \text{ MeV}, \quad E_{\text{sym}} = 31 \text{ MeV}.
\end{aligned} \tag{16}$$

We choose the value of m_0 in the range of 500 – 900 MeV [10]. Since the value of the incompressibility K is relatively not well fixed compared to the other nuclear matter properties, we use two different values of K as inputs. The determined parameters are shown in Table II, where $K = 240$ MeV, and Table III, where $K = 215$ MeV.

TABLE II. Parameter set 1: $K = 240$ MeV.

m_0 (MeV)	600	700	800	900
g_1	14.836	14.171	13.349	12.329
g_2	8.427	7.762	6.941	5.921
$g_{\omega NN}$	9.132	7.305	5.660	3.522
$g_{\rho NN}$	3.927	4.065	4.149	4.218
$\bar{\mu}^2/f_\pi^2$	21.821	18.842	11.693	1.537
λ	39.367	34.584	22.578	4.388
$\lambda_6 f_\pi^2$	15.344	13.540	8.683	0.649
m_σ (MeV)	411.299	385.805	330.440	269.255

We remark here that the coefficient of the six-point interaction of the σ meson is positive, which implies that the potential is not bounded below and the system is

TABLE III. Parameter set 2: $K = 215$ MeV.

m_0 (MeV)	600	700	800	900
g_1	14.836	14.171	13.349	12.329
g_2	8.427	7.762	6.941	5.921
$g_{\omega NN}$	8.902	7.055	5.471	3.389
$g_{\rho NN}$	3.948	4.080	4.157	4.221
$\bar{\mu}^2/f_\pi^2$	23.377	20.980	13.346	2.502
λ	42.369	38.921	26.128	6.673
$\lambda_6 f_\pi^2$	16.790	15.739	10.580	1.969
m_σ (MeV)	413.612	384.428	324.007	257.583

not stable for infinite scalar mean field. However, since the σ field in our model is the chiral partner of the pion field, the mean value of the σ field in dense matter is in general smaller than the one in free space due to (partial) chiral symmetry restoration. Therefore, our system will be stable within the mean field approximation in dense matter. It can be seen from Tables II and III that the couplings of the σ field and ω field to nucleons decrease as m_0 increases, which is consistent with the observation made in Ref. [11].

In Fig. 1 we show nucleon density distribution $n(r)$ in ^{40}Ca and ^{48}Ca calculated with the parameter set 2. From Fig. 1 we observe that the central density tends to increase with m_0 .

Now, we calculate the binding energy and the charge radius of some selected nuclei using the parameter sets. We present our results in Tables IV and V together with the corresponding root-mean-square (RMS) deviations. We have used the experimental values compiled in Refs. [22, 23]. We remark here that we cannot obtain converged numbers in our calculations for several nuclei when $m_0 = 500$ MeV, and therefore we have ruled out the case with $m_0 = 500$ MeV. As it can be seen from Tables IV and V, our results approach the experimental values as m_0 is increased till $m_0 = 700$ MeV and start to deviate more afterwards. From Tables IV and V, we conclude that $m_0 = 700$ MeV is favored by nuclear properties such as the nuclear binding energies and charge radii. We can understand our conclusion from the following two observations. First, from Tables II and III, we can see that the values of $\bar{\mu}^2/f_\pi^2$, λ , and $\lambda_6 f_\pi^2$ decrease slightly as m_0 changes from 600 MeV to 700 MeV, while the values change drastically when m_0 is larger than 700

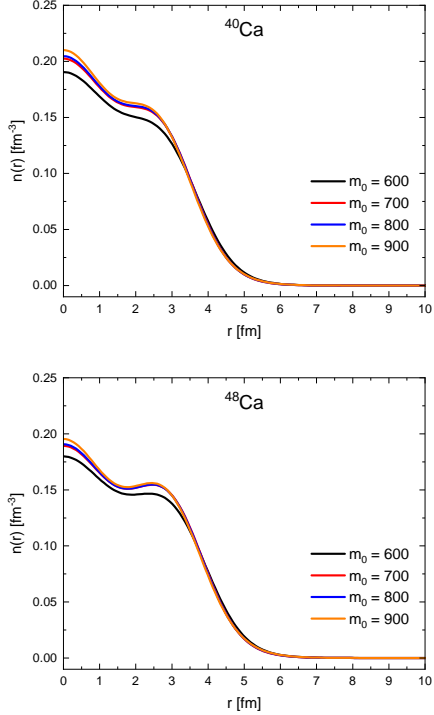


FIG. 1. (Color online) Nucleon density profile in ^{40}Ca and ^{48}Ca calculated with the parameter set 2.

MeV. Second, from Fig. 2 it can be seen that $\langle\omega_0\rangle$ decreases gradually as m_0 increases, while $\langle\sigma\rangle$ shows a peculiar behavior. As m_0 increases from 600 MeV to 700 MeV, $\langle\sigma\rangle$ increases, while the value changes little when m_0 increases from 700 MeV to 800 MeV and then drops when $m_0 = 900$ MeV. From the above observation, we fix

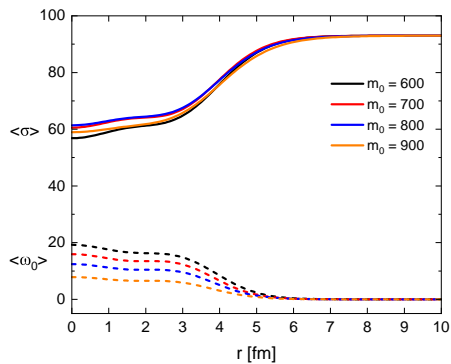


FIG. 2. (Color online) $\langle\sigma\rangle$ and $\langle\omega_0\rangle$ calculated with the parameter set 2 in ^{48}Ca .

the value of the chiral invariant mass as $m_0 = 700$ MeV and try to improve the results of nuclear properties. For

TABLE IV. The binding energy per nucleon and the charge radius (R_C) with the parameter set 1.

m_0 (MeV)		600	700	800	900	Exp.	
BE/A (MeV)	^{16}O	7.087	7.280	6.792	5.093	7.976	
	^{40}Ca	7.736	7.906	7.538	6.191	8.551	
	^{48}Ca	7.676	7.768	7.378	6.061	8.667	
	^{58}Ni	7.391	7.486	7.108	5.849	8.732	
	^{70}Ge	7.761	7.900	7.584	6.429	8.722	
	^{82}Se	7.799	7.899	7.580	6.462	8.693	
	^{92}Mo	7.741	7.821	7.507	6.424	8.658	
	^{112}Sn	7.668	7.760	7.474	6.460	8.514	
	^{126}Sn	7.757	7.801	7.516	6.536	8.443	
	^{138}Ba	7.695	7.758	7.482	6.526	8.393	
R_C (fm)	^{154}Sm	7.596	7.691	7.447	6.540	8.227	
	^{170}Er	7.526	7.587	7.354	6.484	8.112	
	^{182}W	7.418	7.466	7.237	6.387	8.018	
	^{202}Pb	7.277	7.303	7.062	6.221	7.882	
	^{208}Pb	7.306	7.322	7.075	6.232	7.867	
	RMS deviation		0.827	0.737	1.047	2.147	—
	R_C (fm)	^{16}O	2.877	2.792	2.790	2.803	2.699
		^{40}Ca	3.572	3.491	3.485	3.479	3.478
		^{48}Ca	3.605	3.537	3.532	3.522	3.478
		^{58}Ni	3.932	3.863	3.861	3.855	3.776
^{70}Ge		4.104	4.028	4.018	4.001	4.041	
^{82}Se		4.223	4.154	4.145	4.125	4.140	
^{92}Mo		4.418	4.351	4.347	4.335	4.315	
^{112}Sn		4.684	4.616	4.608	4.591	4.594	
^{126}Sn		4.764	4.703	4.695	4.675	4.685	
^{138}Ba		4.928	4.865	4.856	4.834	4.838	
RMS deviation	^{154}Sm	5.117	5.045	5.031	5.004	5.105	
	^{170}Er	5.250	5.181	5.169	5.144	5.279	
	^{182}W	5.374	5.305	5.294	5.270	5.356	
	^{202}Pb	5.555	5.493	5.485	5.462	5.471	
	^{208}Pb	5.588	5.529	5.521	5.499	5.501	
	RMS deviation		0.097	0.052	0.053	0.062	—

this we use the following nuclear matter properties

$$\begin{aligned} \frac{E}{A} - m_N &= -16.3 \text{ MeV}, & n_0 &= 0.16 \text{ fm}^{-3}, \\ K &= 215 \text{ MeV}, & E_{\text{sym}} &= 30 \text{ MeV}, \end{aligned} \quad (17)$$

and determine our model parameters again, which are given in Table VI. With this new parameter set, we calculate the properties of selected nuclei and compare our results with experiments in Table VII, where the RMS deviation of our results is 0.204 for the binding energy and 0.045 for the charge radius. As in Table VII, our results are in quantitative agreement with experiments. To see how our results compare with the ones from a Walecka-type mean field model, we also show the results from, for example, the spherical relativistic continuum Hartree-Bogoliubov (RCHB) theory with the relativistic

TABLE V. The binding energy per nucleon and the charge radius (R_C) with the parameter set 2.

m_0 (MeV)		600	700	800	900	Exp.
BE/A (MeV)	^{16}O	7.489	7.781	7.298	5.698	7.976
	^{40}Ca	8.063	8.301	7.942	6.693	8.551
	^{48}Ca	7.978	8.134	7.757	6.541	8.667
	^{58}Ni	7.685	7.841	7.473	6.308	8.732
	^{70}Ge	8.044	8.239	7.932	6.866	8.722
	^{82}Se	8.066	8.219	7.910	6.881	8.693
	^{92}Mo	7.993	8.123	7.822	6.828	8.658
	^{112}Sn	7.911	8.050	7.774	6.844	8.514
	^{126}Sn	7.980	8.070	7.802	6.909	8.443
	^{138}Ba	7.920	8.028	7.764	6.890	8.393
	^{154}Sm	7.821	7.958	7.724	6.894	8.227
	^{170}Er	7.733	7.837	7.618	6.830	8.112
	^{182}W	7.616	7.707	7.494	6.726	8.018
	^{202}Pb	7.468	7.535	7.310	6.549	7.882
^{208}Pb	7.496	7.552	7.321	6.558	7.867	
RMS deviation		0.573	0.438	0.727	1.734	—
R_C (fm)	^{16}O	2.845	2.763	2.772	2.796	2.699
	^{40}Ca	3.546	3.469	3.473	3.479	3.478
	^{48}Ca	3.585	3.521	3.525	3.527	3.478
	^{58}Ni	3.912	3.848	3.856	3.863	3.776
	^{70}Ge	4.085	4.013	4.013	4.008	4.041
	^{82}Se	4.209	4.145	4.144	4.135	4.140
	^{92}Mo	4.401	4.339	4.344	4.344	4.315
	^{112}Sn	4.671	4.608	4.609	4.602	4.594
	^{126}Sn	4.754	4.697	4.698	4.688	4.685
	^{138}Ba	4.920	4.862	4.861	4.849	4.838
	^{154}Sm	5.111	5.045	5.039	5.022	5.105
	^{170}Er	5.242	5.178	5.175	5.160	5.279
	^{182}W	5.364	5.301	5.298	5.286	5.356
	^{202}Pb	5.549	5.493	5.493	5.481	5.471
^{208}Pb	5.584	5.531	5.532	5.519	5.501	
RMS deviation		0.082	0.046	0.049	0.056	—

density functional PC-PK1 [23, 24]. Using the parame-

TABLE VI. Parameter set 3. All parameters are dimensionless except m_σ .

g_1	g_2	$g_{\omega NN}$	$g_{\rho NN}$	$\bar{\mu}^2/f_\pi^2$	λ	$\lambda_6 f_\pi^2$	m_σ [MeV]
14.171	7.762	7.036	3.958	21.135	39.332	15.996	382.140

ter set 3, we finally calculate the r -dependence of neutron and proton masses which are given by Eq. (6) with the r -dependent $\langle\sigma\rangle$, and present our results in Fig. 3. Our results show that, as expected, the neutron-proton mass difference is larger in the nuclear system with a larger isospin asymmetry.

TABLE VII. The binding energy per nucleon and the charge radius (R_C) with the parameter set 3.

	BE/A (MeV)			R_C (fm)		
	PDM	RCHB	Exp.	PDM	RCHB	Exp.
^{16}O	8.040	7.956	7.976	2.757	2.768	2.699
^{40}Ca	8.574	8.577	8.551	3.464	3.481	3.478
^{48}Ca	8.419	8.654	8.667	3.517	3.494	3.478
^{58}Ni	8.118	8.691	8.732	3.843	3.737	3.776
^{70}Ge	8.521	8.650	8.722	4.010	4.001	4.041
^{82}Se	8.513	8.664	8.693	4.142	4.125	4.140
^{92}Mo	8.408	8.662	8.658	4.335	4.310	4.315
^{112}Sn	8.339	8.489	8.514	4.605	4.582	4.594
^{126}Sn	8.372	8.447	8.443	4.695	4.683	4.685
^{138}Ba	8.329	8.406	8.393	4.860	4.848	4.838
^{154}Sm	8.263	8.149	8.227	5.042	5.062	5.105
^{170}Er	8.140	8.000	8.112	5.176	5.224	5.279
^{182}W	8.007	7.927	8.018	5.299	5.342	5.356
^{202}Pb	7.837	7.869	7.882	5.491	5.490	5.471
^{208}Pb	7.860	7.875	7.867	5.529	5.518	5.501
RMS deviation	0.204	0.05	—	0.045	0.031	—

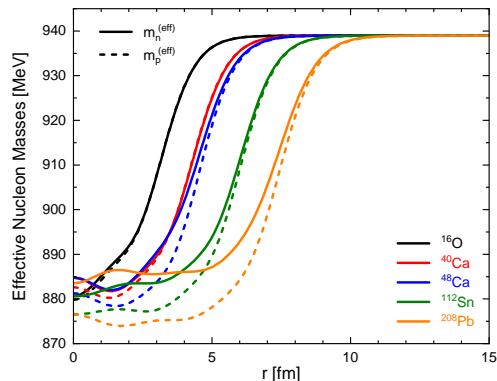


FIG. 3. (Color online) The neutron and proton masses in a nucleus calculated with the parameter set 3.

IV. SUMMARY

In this work, using the extended parity doublet model [10], we calculated the properties of some stable nuclei in the mean field approximation to estimate the value of the chiral invariant mass preferred by nuclear properties. Since our primary goal in this work is to see if the parity doublet model can explain some basic nuclear properties such as the binding energy, we didn't consider pairing correlations which are essential for odd-even staggering in nuclear properties. We observed that our results are closest to the experiments when we take $m_0 = 700$ MeV. Therefore, we have concluded that the

chiral invariant mass contribution to the nucleon mass is around 700 MeV, which can be understood from the peculiar behavior of $\bar{\mu}^2/f_\pi^2$, λ , $\lambda_6 f_\pi^2$, $\langle\sigma\rangle$, and $\langle\omega_0\rangle$ as the value of m_0 changes. We also calculated the neutron and proton masses in a nucleus and observed that the neutron-proton mass difference becomes larger in a isospin asymmetric nucleus.

In the future we will extend our present study by including pairing correlations and deformations using more complete approaches such as (deformed) RCHB theory which can provide an appropriate treatment of the pairing correlation in the presence of the continuum through the Bogoliubov transformation in a microscopic and self-

consistent way [25].

ACKNOWLEDGMENTS

We thank Jie Meng for providing the RCHB code. This work was supported in part by the Rare Isotope Science Project of Institute for Basic Science funded by Ministry of Science and ICT and National Research Foundation of Korea (2013M7A1A1075764), by the Institute for Basic Science (IBS-R031-D1), by National Research Foundation of Korea (NRF) grants funded by the Korean government (Ministry of Science and ICT) (No. 2021R1F1A1060066, No.2020R1A2C3006177), and by JPSP KAKENHI Grant Number 20K03927.

-
- [1] C. E. Detar and T. Kunihiro, Phys. Rev. D **39**, 2805 (1989).
 - [2] T. Hatsuda and M. Prakash, Phys. Lett. B **224**, 11 (1989).
 - [3] D. Zschiesche, L. Tolos, J. Schaffner-Bielich and R. D. Pisarski, Phys. Rev. C **75**, 055202 (2007).
 - [4] V. Dexheimer, S. Schramm and D. Zschiesche, Phys. Rev. C **77**, 025803 (2008).
 - [5] C. Sasaki and I. Mishustin, Phys. Rev. C **82**, 035204 (2010).
 - [6] S. Gallas, F. Giacosa and G. Pagliara, Nucl. Phys. A **872**, 13 (2011).
 - [7] C. Sasaki, H. K. Lee, W. G. Paeng and M. Rho, Phys. Rev. D **84**, 034011 (2011).
 - [8] J. Steinheimer, S. Schramm and H. Stoecker, Phys. Rev. C **84**, 045208 (2011).
 - [9] S. Benic, I. Mishustin and C. Sasaki, Phys. Rev. D **91**, no. 12, 125034 (2015).
 - [10] Y. Motohiro, Y. Kim and M. Harada, Phys. Rev. C **92**, no. 2, 025201 (2015); Erratum: [Phys. Rev. C **95**, no. 5, 059903 (2017)]
 - [11] M. Harada and T. Yamazaki, "Charmed Mesons in Nuclear Matter Based on Chiral Effective Models," JPS Conf. Proc. **26**, 024001 (2019).
 - [12] M. Bender, P. H. Heenen and P. G. Reinhard, Rev. Mod. Phys. **75**, 121 (2003).
 - [13] D. Vretenar, A. V. Afanasjev, G. A. Lalazissis and P. Ring, Phys. Rept. **409**, 101 (2005).
 - [14] J. Meng, H. Toki, S. G. Zhou, S. Q. Zhang, W. H. Long and L. S. Geng, Prog. Part. Nucl. Phys. **57**, 470 (2006).
 - [15] *Relativistic Density Functional for Nuclear Structure*, International Review of Nuclear Physics, Vol. 10, edited by J. Meng (World Scientific, Singapore, 2016).
 - [16] *Energy Density Functional Methods for Atomic Nuclei*, edited by N. Schunck (IOP Publishing Ltd 2019).
 - [17] D. Jido, M. Oka and A. Hosaka, Prog. Theor. Phys. **106**, 873 (2001).
 - [18] S. Gallas, F. Giacosa and D. H. Rischke, Phys. Rev. D **82**, 014004 (2010).
 - [19] W. G. Paeng, H. K. Lee, M. Rho and C. Sasaki, Phys. Rev. D **85**, 054022 (2012).
 - [20] M. Bando, T. Kugo and K. Yamawaki, Phys. Rept. **164**, 217 (1988).
 - [21] M. Harada and K. Yamawaki, Phys. Rept. **381**, 1 (2003).
 - [22] M. Wang *et al.*, Chin. Phys. C **36**, 1603 (2012).
 - [23] X. W. Xia *et al.*, Atom. Data Nucl. Data Tabl. **121-122**, 1 (2018).
 - [24] P. W. Zhao, Z. P. Li, J. M. Yao and J. Meng, Phys. Rev. C **82**, 054319 (2010).
 - [25] J. Meng and S. G. Zhou, J. Phys. G **42**, no. 9, 093101 (2015).